FLOMEKO2019
18th International Flow Measurement Conference
Portugal | Lisbon | LNEC | 26-28 june 2019

Uncertainty of SO2 measurements in dryers due to water droplet and water film condensation

S. Knotek[1], J. Geršl[1], A. Paták[2]

[1]Czech Metrology Institute, Brno, Czech Republic
[2]Institute of Scientific Instruments of the Czech Academy of Sciences, Brno, Czech Republic
E-mail (corresponding author): sknotek@cmi.cz

Abstract

The article presents the modeling of SO_2 diffusion into water droplet and water film which arise in dryers by condensation or evaporation in dependence on physical and chemical conditions. The motivation of the modeling is the attempt to quantify the SO_2 loses in drying during sampling of emissions. The basic processes of gaseous substances dissolution into liquid are discussed theoretically and quantitative results of computer computations are presented.

1. Introduction

The SO_2 pollution of air has a significant impact on health of the population in long-term as well as in short-term period [1]. Since most of the atmospheric SO_2 is produced by industrial processes, the accurate measurement of emissions is needed.

Nowadays, the Standard Reference Methods (SRMs) used for measuring of emissions are based on laboratory analysis of solution which is received by dissolution of stack gas passing through a series of glass impingers filled with H_2O_2(aq). Thus, the concentration of SO_2 in stack gas is related to the amount of corresponding sulphate. Since this attitude contributes to the uncertainty of the measurement, needs other calibrations and also does not allow automated monitoring of emissions, other attitudes are being sought. One of the possible measuring approaches with required uncertainty are portable automated measuring systems (P-AMSs), see Figure 1. However, these P-AMSs are able to measure only filtered and dried stack gas. Since the sulfur dioxide is soluble in water, the amount of SO_2 removed from stack air during process of drying should be described. The aim of this article is an attempt to summarize an appropriate mathematical model.

2. Theoretical background

Two basic phenomena need to be taken into account in modeling of removing gaseous substances during drying process. Since the gas is dissolved in liquid water, the condensation processes are needed to be described in dependence on the physical and geometrical conditions. Once the microscopic liquid phase of water occurs in the dryer (in form of water film or water droplet), the transfer of gaseous soluble species into water is driven by diffusion processes simultaneously with the continuing condensation of water.

Figure 1: Portable gas conditioning unit. Taken from **[2]**.

The dropwise or filmwise condensation of water can proceed simultaneously or one of the process can prevail. The dropwise condensation obviously occurs in atmosphere on nucleus of dust, while the filmwise condensation prevails on hydrophilic surfaces with temperature under the saturation temperature (in multicomponent vapor called dew point). Both processes are supposed to proceed in dryers of P-AMSs since small nucleus can probably still occur in filtered stack gas and the gas cooler inside P-AMSs, see the scheme in Figure 2, is based on subcooling of glas walls to defined temperature deeply under the saturation temperature. Thus, both of the condensation processes are outlined in following paragraphs.

2.1. Droplet growth by condensation

The mathematical description of droplet growth is studied in theory of aerosols, e.g. in [3].

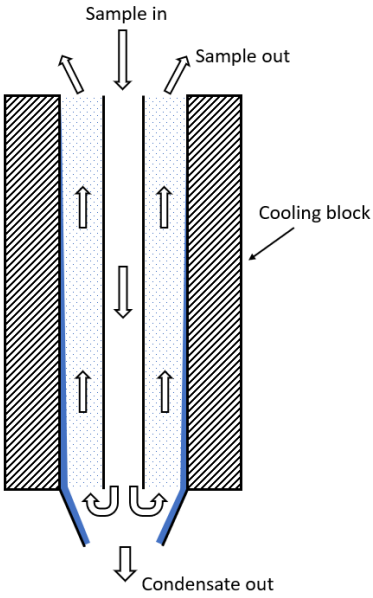

Figure 2: Schemes of the condensation in dryer.

The condensation processes in humid air depends on the saturation ratio (multiplied by 100% known as relative humidity) of the partial pressure of water vapor to the saturation vapor pressure

$$S_R = \frac{p}{p_s} \tag{1}$$

The saturation water vapor pressure for a plane liquid surface is given by empirical formula

$$p_s = \exp\left(16.7 - \frac{4060}{T - 37}\right) \tag{2}$$

where T is the absolute temperature in K and p_s is the saturation pressure in kPa.
In case of the planar surface water begins to condense if $S_R = 1$. However, the saturation ratio, called the Kelvin ratio K_R, in case of microscopic water droplets is given by the Kelvin or Thomson-Gibbs equation

$$K_R = \frac{p_d}{p_s} = \exp\left(\frac{4\gamma M}{\rho R T d}\right) \tag{3}$$

where γ, M, ρ and R are the surface tension, molecular weight, density of the liquid and universal gas constant, respectively, p_d is partial pressure at the surface of the droplet with diameter d. Since the argument of exponential function in (3) is always positive, the right-hand side of (3) is always bigger than one. It means that for the equilibrium state (droplet diameter remains the same) the saturation ratio needs to be bigger than for flat surface. This is caused by the strongly curved surface from which molecules escape easier than from flat surface. According to the formula, the smaller diameter of the droplet the bigger partial pressure is needed for the equilibrium state. Theoretically saturation ratio of 220 would be needed for the growth of an individual molecule. However in reality, the droplet growth starts from the cluster of several molecules which are established due to van der Waals forces. From the other direction, the saturation ratio is close to unity for droplet diameter bigger than 0.1 μm ($K_R = 1.044$ for $d = 0.05$ μm at 293 K).

Once a stable nucleus of droplet is established, i.e. the diameter of nucleus is bigger than d given by formula (3) for a given saturation ratio (or reversely saturation ratio is bigger than K_R given by formula (3) for a given nucleus diameter), the droplet begins to growth. In [3] two formulae in dependence on the current diameter are derived. When the droplet diameter is less than gas mean free path, λ, the formula has the form

$$\frac{\mathrm{d}(d_p)}{\mathrm{d}t} = \frac{2M\alpha(p_\infty - p_d)}{\rho N_A \sqrt{2\pi m k T}} \quad \text{for } d_p < \lambda \tag{4}$$

where α is accommodation coefficient, p_∞ is partial pressure far from the droplet surface, p_d is partial pressure of vapor at the droplet surface given by Kelvin equation (3), N_A is Avogadro constant, $m = M/N_A$ is mass of vapor molecule and $k = 1.3806485 \cdot 10^{-23}$ is Boltzmann constant.

In case the droplet is bigger than mean free path, the formula becomes

$$\frac{\mathrm{d}(d_p)}{\mathrm{d}t} = \frac{4DM}{R\rho d_p}\left(\frac{p_\infty}{T_\infty} - \frac{p_d}{T_d}\right)\phi \quad \text{for } d_p > \lambda \tag{5}$$

where D is diffusion coefficient of water vapor, ϕ is the Fuchs correction factor significant for particles less than 1μm, p_d is vapor partial pressure near the droplet surface which can be calculated by formula (3) and finally the droplet temperature T_d can be computed using ambient temperature T_∞ by

$$T_d = T_\infty + \frac{(6.65 + 0.345T_\infty + 0.0031T_\infty^2)(S_R - 1)}{1 + (0.082 + 0.00782T_\infty)S_R} \tag{6}$$

where T_∞ in ratio needs to be in °C.

Since gas mean free path is quite small in comparison to final droplet diameters, the amount of dissolved SO_2 is not affected by the initial droplet growth described by equation (4). Moreover, since the expected final droplet

diameters are much bigger than 1 μm, we will approximate the droplet growth by eq. (5) for $\phi = 1$. After integration of (5) we get the prescription for droplet diameter in time by

$$d_p(t) = \sqrt{\frac{8DM}{R\rho}\left(\frac{p_\infty}{T_\infty} - \frac{p_d}{T_d}\right)(t - t^0) + \left(d_p^0\right)^2} \qquad (7)$$

where d_p^0 is initial droplet diameter in time t^0. Temporal evolution of droplet diameter for different relative humidity can be seen in Figure 3.

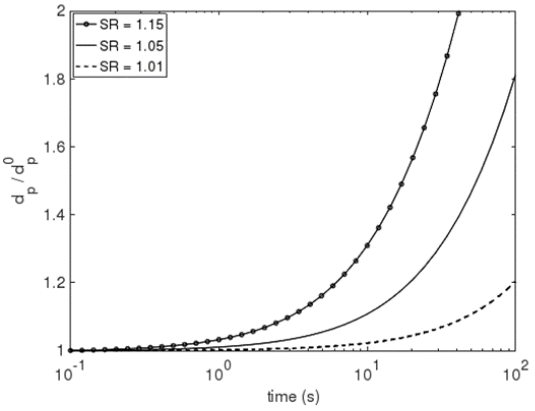

Figure 3: Temporal evolution of the droplet diameter in dependence on the saturation ratio (relative humidity).

2.2 Liquid film condensation

The liquid film occurs in case when a saturated or superheated vapor is located near the object (wall) that has the temperature lower than the corresponding saturation temperature. Authors in [4] distinguish heterogeneous nucleation which occurs at the solid-liquid interface and homogeneous nucleation which is the name for the case when growing droplet occurs entirely in the supercooled water as was described in the previous paragraph. In case of heterogeneous nucleation, the wettable surface leads to the filmwise condensation while the hydrophobic surface leads to the dropwise condensation, see Figure 4. Supposing that the glass of the cooler in P-AMSs is hydrophilic, we will focus in the next text on the filmwise condensation.

The classical analysis of laminar film on inclined or vertical wall is known from Nusselt (1916). Since the film covers whole surface, the condensation process is pushed by the heat transfer between the vapor and wall. Following from the Fourier's Law and supposing some assumptions (laminar flow, stagnant liquid vapor, smooth liquid film surface, etc. see [4]), the following formula (8) for liquid film thickness, δ, can be derived.

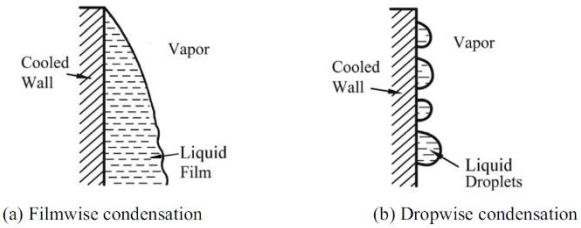

Figure 4: Heterogeneous condensation. Taken from **[4]**.

$$\delta(x) = \left(\frac{4k_l\mu_l x\Delta T}{\rho_l(\rho_l - \rho_v)gh_{lv}}\right)^{1/4} \qquad (8)$$

where k_l is thermal conductivity of the liquid, μ_l and ρ_l are dynamic liquid viscosity and liquid density, ρ_v is vapor density, x is coordinate in the wall direction and h_{lv} is latent heat of the liquid-vapor phase change.

As was mentioned above, the Nusselt theory has been derived for laminar flow regime and the vertical configuration. However, as the condensation proceeds, more and more liquid flows down due to gravity and becomes unstable. At first small waves are established on the liquid film surface and if the wall is long enough, the irregular waves called ripples can appear and the turbulent regime can be achieved. Unfortunately, no standardized theory has been approved for unstable regimes and the numerical attitudes are often need to be used.

The flow regime can be determined using the Reynolds number defined in [4] as

$$Re = \frac{4\rho_l(\rho_l - \rho_v)g\delta^3}{3\mu_l^2} \qquad (9)$$

The flow regime changes from laminar to wavy around Re=30 and becomes turbulent for approximately Re=1800 [4].

Note that in the previous text it was assumed that the vapor is stagnant. As follows from the design of P-AMSs, the film is supposed to flow downward due to gravity, while stack gas is flowing upward through the cooler, see Figure 2. We speak about countercurrent vapor flow and the motion of gas needs to be taken into account. Authors in [4] show that a nonlinear system of governing equations is derived if a shear stress from vapor motion is supposed on the liquid film interface. The corresponding mechanistic models are outlined in [5], [6] or [7]. Numerical implementation using finite volume methods can be found in [8] or [9].

Other attitude is based on the theory of heat exchanger design, see e.g. in [10]. In this case the reverse value of the overall heat transfer coefficient, $\bar{h}$, is found as the sum of the heat resistances for the appropriate heat exchanger. From the heat and mass balance the amount of condensate can be estimated. However, since the liquid film becomes thicker with increasing condensation and the flow regime can change along the wall, the division into several zones should be taken into account in this attitude.

2.3 Effect of noncondensable gas

Near the liquid film exists a boundary layer in which the partial pressure of the condensable vapor decreases from $p_{v\infty}$ far from the interface to $p_{v\delta}$ at the interface. On the other hand, the partial pressure of the noncondensable gas increases according to Dalton's law of partial pressure.

$$p = \sum p_i \tag{10}$$

Since the partial pressure of the condensable gas decreases, the corresponding saturation temperature decreases as well and hence the temperature at the gas-liquid interface, T_δ, can be much lower than in case of pure vapor. According to [4], in case of small inert gas content, this temperature can be computed using equation (11), where h_g and h_l are heat transfer coefficients in gas and liquid phase, respectively.

$$T_\delta - T_w = \frac{h_g}{h_l}\left[\frac{h_{lv}}{c_{pg}} \ln \frac{p - p_{v\delta}}{p - p_{v\infty}}\right] \tag{11}$$

2.4 Mass transfer through gas-liquid interface

According to the *Henry's law* in form

$$n_l = H^{cp}\, p_i \tag{12}$$

the concentration of a species in the aqueous phase, n_l, is proportional to the partial pressure of this matter in the gas phase, p_i . H^{cp} is the *Henry's law constant* in $\mathrm{mol \cdot m^{-3} \cdot Pa^{-1}}$. Note that there are several other definitions of Henry's law constant. The dimensionless form is given by

$$H^{cc} = \frac{n_l}{n_g} \tag{13}$$

The conversion between H^{cc} and H^{cp} for ideal gas is

$$H^{cc} = H^{cp} R\, T \tag{14}$$

where R is the universal gas constant.

Due to this limitation of maximal concentration in liquid, the solution through the interface is not continuous as it is for example in the problem of heat conduction which is represented by the same differential equation. The dependence of Henry's law constant on temperature can be extrapolated from a single data point applying van't Hoff equation by formula

$$H(T) = H^0 \exp\left[-\frac{\Delta h}{R}\left(\frac{1}{T} - \frac{1}{T^0}\right)\right] \tag{15}$$

where H^0 is Henry's law constant in temperature T^0 and Δh is enthalpy change due to transport of soluble gas substance into liquid. The dependence of Henry's law constant on temperature and independence on pressure have been confirmed in [11]. The values of Henry's law constant for different substances and water as solvent can be found in [12].

The ratio of molecules absorbed through the gas-liquid interface to the number of molecules which hit the liquid surface is given by the *mass accommodation coefficient*, α. As has been shown in [13] using the comparison of characteristic times of different processes, the droplet surface is saturated faster than equilibrium state can be established due to diffusion. This leads to the re-evaporation of some molecules from interface and the resulting ratio of absorbed molecules can be described using the mass accommodation coefficient. The experimental measurements of mass accommodation coefficient of SO_2 at the air-water interface are presented in [13] and [14]. The authors report measurements of $\alpha = (6.0 \pm 0.8) \cdot 10^{-2}$ at 298 K and $\alpha = (5.4 \pm 0.6) \cdot 10^{-2}$ at 295 K, respectively.

2.5 Physical and chemical processes in liquid phase

Experimental observations in [13] show that the mass accommodation coefficient is strongly dependent on pH and real solubility at the droplet surface. For considering of these dependencies, the chemical processes in liquid need to be take into account. According to [15], the following chemical reactions occur if SO_2 is dissolved in water

$$\mathrm{SO_2(g) + H_2O} \xrightarrow{K_H} \mathrm{SO_2 \cdot H_2O}\,, \tag{16}$$

where $K_H = \frac{[\mathrm{SO_2 \cdot H_2O}]}{p_{\mathrm{SO_2}}}$

$$\mathrm{SO_2 \cdot H_2O} \xrightarrow{K_1} \mathrm{H^+ + HSO_3^-}\,, \tag{17}$$

where $K_1 = \frac{[\mathrm{H^+}][\mathrm{HSO_3^-}]}{[\mathrm{SO_2 \cdot H_2O}]}$

$$\mathrm{HSO_3^-} \xrightarrow{K_2} \mathrm{H^+ + SO_3^{2-}}\,, \tag{18}$$

where $K_2 = \frac{[\mathrm{H^+}][\mathrm{SO_3^{2-}}]}{[\mathrm{HSO_3^-}]}$.

Note that $[\cdot]$ represents the concentration, K_H is the Henry's constant H^{cp}, K_1 and K_2 are the first and the second dissociation constants. The total concentration of the dissolved sulfur with oxidation number four can be calculated as the sum

$$[S(IV)] = [\mathrm{SO_2 \cdot H_2O}] + [\mathrm{HSO_3^-}] + [\mathrm{SO_3^{2-}}] \quad (19)$$

Following the considerations in previous paragraph, the equilibrium state of the sulfur dioxide concentration inside the droplet can be expressed by

$$n_l = H^{cp,*}_{S(IV)} p_{\mathrm{SO_2}}\,, \quad (20)$$

where $H^{cp,*}_{SO_2}$ is the effective Henry's constant computed by formula

$$H^{cp,*}_{S(IV)} = H^{cp}_{SO_2}\left(1 + \frac{K_1}{[\mathrm{H^+}]} + \frac{K_1 K_2}{[\mathrm{H^+}]^2}\right), \quad (21)$$

where concentration $[\mathrm{H^+}]$ is connected with pH scale by

$$\mathrm{pH} = -\log[\mathrm{H^+}]\,, \quad (22)$$

where $[\mathrm{H^+}]$ needs to be in mol/dm^3.

Note that neglecting the second dissociation term $[\mathrm{SO_3^{2-}}]$ which has very low concentration, the effective Henry's law constant can be expressed using substitution of (14) and (15) into (19) by

$$H^{cp,*}_{S(IV)} = K_H + \sqrt{\frac{K_H K_1}{p_{\mathrm{SO_2}}}} \quad (23)$$

As well as the Henry's law constant also the dissociation constants are dependent on temperature. According to experimental data, authors in [16] proposed correlations

$$\ln K_H = -\frac{3715.2}{T} + 16.765 \quad (24)$$

$$\ln K_1 = \frac{1447.1}{T} - 9.11 \quad (25)$$

Using equation (23) and formulas (24-25) authors of [16] derived equation for total concentration of sulfur dioxide absorbed in water in dependence on temperature, see formula (26). The corresponding concentration of SO_2 which can be absorbed from air with initial concentration of 0.01 ppm in dependence on temperature can be seen in Figure 5.

$$[S(IV)] = 2.407 \cdot 10^{-6} \cdot \left[0.0218 \cdot \exp\left(\frac{3715.2}{T}\right) p + \exp\left(\frac{2581.1}{T}\right) p^{0.5}\right] \quad (26)$$

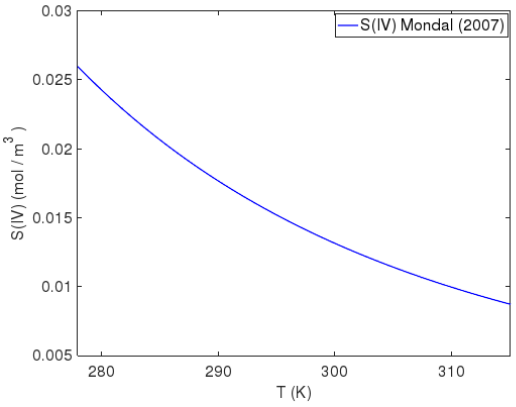

Figure 5: Total SO_2 absorbed in water in dependence on temperature. Initial SO_2 concentration in air 0.01ppm.

2.6 Diffusion

The diffusion processes are described by equation

$$\frac{\partial n(x,t)}{\partial t} = \frac{\partial}{\partial x}\left(D\frac{\partial n(x,t)}{\partial x}\right) \quad (27)$$

where $n(x,t)$ is concentration in position x and time t and D is the diffusion coefficient. Since the studied phenomenon needs to be solved as coupled system for both phases, the system of two coupled diffusion equations for constant diffusion coefficients takes the form

$$\frac{\partial n_g(x,t)}{\partial t} = D_g \frac{\partial^2 n_g(x,t)}{\partial x^2} \quad (28)$$

$$\frac{\partial n_l(x,t)}{\partial t} = D_l \frac{\partial^2 n_l(x,t)}{\partial x^2} \quad (29)$$

The dependence of diffusion coefficient of SO_2 in water on temperature and pH is presented in [17]. The influence on temperature is given by

$$D_l = -1.21 \cdot 1010^{-3} + 4.33 \cdot 10^{-6} \cdot T \quad (30)$$

Analytical solutions of equations (28) and (29) for different geometrical configurations and different boundary conditions are given in [18]. However, the presented suitable solutions do not take into account the Henry's law which limits the maximal concentration of

dissolved substance in liquid and the mass accommodation coefficient which defines the fraction of molecules entering through the gas-liquid interface. The boundary conditions which take into account the Henry's Law and accommodation coefficient are presented in [19] by forms

$$-D_g \frac{\partial}{\partial x} n_g(x_i,t) = \frac{\alpha\,\bar{v}}{4}\left(n_g(x_i,t) - \frac{n_l(x_i,t)}{H^{cc}}\right), \quad (31)$$

$$-D_l \frac{\partial}{\partial x} n_l(x_i,t) = \frac{\alpha\,\bar{v}}{4}\left(n_g(x_i,t) - \frac{n_l(x_i,t)}{H^{cc}}\right), \quad (32)$$

where x_i is the location of the gas-liquid interface and $\bar{v}$=300 m/s is mean thermal velocity of SO_2 as given by [20].

3. Solution notes

Fairly comprehensive attitude to the modeling of soluble gas transport into large droplets during evaporation and condensation is presented in [15] and [21]. Rather complex numerical solution of the presented differential equations with moving boundaries led to the idea of using the tool based on finite element (FEM) or finite volume method (FVM) using Fluent [22]. The attitude with global heat transfer coefficient computed using correlation of Nusselt dimensionless numbers is used in [23]. Although some research articles can be found for each of the aforementioned phenomena, there is a lack of studies dealing with the analysis of SO_2 in dryers of P-AMS type as well as with analysis of gas dissolution in simultaneously condensing liquid.

Since number of different processes (convection, diffusion, chemical reactions, moving gas-liquid interface etc.) makes the solution quite complex from its nature, the problem seems to be still not well implemented in modern tools for computational fluid dynamic. Thus, the step by step written mathematical model seems to be needed. However, regarding to the geometry and physical configuration of the supposed dryer, the estimate of maximal concentrations can be done separately using model of diffusion into the growing droplet and into the condensing film. In case of droplet the simultaneous simulation of diffusion and droplet growth need to be done. The results using FEM tool are presented in Figures 6. The model is based on equations (28-29) with boundary conditions (31-32) prescribed on gas-liquid interface. The mass accommodation coefficient is set to 0.054, the effective Henry's law constant is computed using (23) where dissociation constants K_H and K_1 are taken from [16], see formula (24-25) . The droplet growth is defined by formula (7) where droplet temperature is prescribed by formula (6), vapor partial pressure is computed by equation (3) and saturation pressure is given by (2).

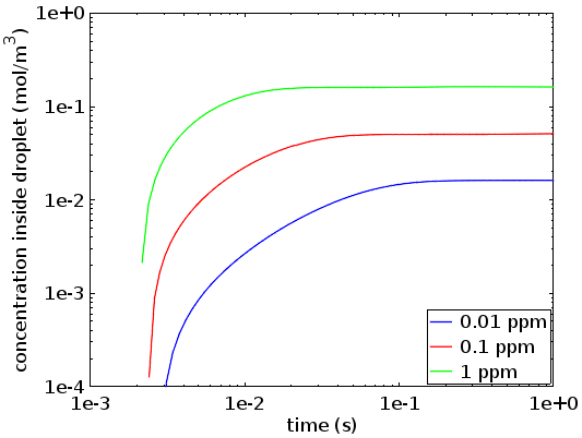

Figure 6: Concentration of SO_2 in growing droplet during time for different values of SO_2 concentration in air with relative humidity equal to 101% and temperature 20°C.

The figure 6 shows the concentration of SO_2 in growing droplet in dependence on the relative humidity. Depending on the initial concentration of SO_2 in gas, the time needed to reach the maximal concentration, which is given by formula (26), ranges between 0.02 and 0.2s. Regarding the dimensions of condensation tubes in P-AMSs (diameter of the tube from 6mm, height from 125 mm) and flow velocity of sampled air, we can suppose, that the maximal concentration can be reached before the droplet is attached to the liquid film on the wall. On the other hand, the droplets are established only in case the relative humidity is bigger than 100%. In other cases, the condensation on the cooled wall with temperature 5°C is predominant for the drying processes in the dryer. Hence, the modeling of liquid film formation due to condensation and corresponding SO_2 dissolution is important for total amount of dissolved SO_2.

In contrast to the growing droplet, in case of the condensing liquid film, the corresponding analysis can be done for a given film thickness, if we can suppose that in process of measurement a stagnant liquid film is established. Hence, although the stationary liquid film thickness can be taken into account, the mathematical models suffer from other complications such as the modeling of interfacial friction or liquid velocity on the film surface in case of moving vapor in dryer when the formula (8) cannot be used. Authors in [6] note two effects of increasing vapor flow on the heat transfer. As can be supposed, the bigger interfacial shear stress leads to the decreasing of the film velocity and increasing film thickness. Bigger film thickness itself would lead

to bigger heat transfer resistance and decreasing condensation rate. However, the increasing interfacial shear stress influences the interfacial perturbations and leads the reinforcement of the turbulence in the liquid film. Bigger turbulence leads to increase of heat transfer. Both effects apply differently in dependence on the value of the film Reynolds number, thus the detailed analysis is needed.

In case of a typical P-AMS, the maximum gas volume flow rate is 150 Nl/h. For a tube with diameter 6mm, this corresponds to gas velocity of about 0.4m/s and laminar flow regime. Supposing limited influence of this laminar flow on the liquid film, the classical Nusselt formula (8) can serve as a basic estimate of the liquid film thickness along the dryer and the liquid volume in which the gas can diffuse. Supposing the length of the dryer tube 0.15m with diameter 0.006m and standard physical properties of water, the film thickness using (8) equals about 0.1 mm for saturation temperature of about 290K. As in the case of water droplet, several FEM simulations have been done using the theoretical basis outlined in the previous chapter. The main difference was the stagnant interface between liquid and gas phase and resolution of convection using the assumptions of laminar flow regimes in both phases. The constant film thickness of 0.1mm have been defined along the 0.15m long dryer. Zero flux of SO_2 has been prescribed in the upper boundary of liquid film and on the wall. The boundary conditions (31-32) have been prescribed on the gas-liquid interface.
The resulting ratios of outlet to inlet SO_2 concentrations in gas for different average velocity of gas flow and different inlet concentrations can be read in Table 1.

Table 1: SO_2 concentration after passing through the cooler with constant water film thickness. Resulting values are normalized to the initial concentration before entrance to the cooler.

	n_g^{SO2} =1 ppm	n_g^{SO2} =10ppm	n_g^{SO2} =100ppm
U_g=0.4 m/s	46.9 %	48.4 %	52.4 %
U_g=0.2 m/s	28.6 %	29.9 %	33.8%
U_g=0.1 m/s	12.6 %	13.4 %	16.0 %

The resulting dependencies in Table 1 show that the SO_2 loses increase with decreasing gas velocity and decreasing SO_2 concentration in gas phase. The loses increase only slightly for lower inlet concentrations, while the dependence on the gas velocity is much more significant. This result is related to the fact, that in case of low gas velocity the dissolving species has more time to diffuse into the water film. Although, the tendencies just presented makes the physical sense, note that a more detailed numerical analysis is needed for credibility of quantitative results.

7. Conclusion

The article summarizes the mathematical models of the main processes crucial for the assessing of SO_2 loses during drying processes in P-AMSs. The models of droplet growing and liquid film formation during condensation have been presented on basis of theoretical as well as experimental findings published in literature. The molecular transport of condensable gas has been discussed with regards to the molecular processes on gas-liquid interface as well as with regards to chemical processes inside liquid. The governing equations of diffusion processes have been presented and the significant boundary condition has been defined using physical parameters from previous sections. The concentrations of SO_2 dissolved in one droplet have been computed using presented mathematical model of diffusion simultaneously with modeling of droplet growth. The average concentration of SO_2 in gas flow leaving the dryer has been simulated for stagnant film thickness, but as well as for droplet using aforementioned diffusion model based on Henry's law theory and chemical reactions connected with dissolution of SO_2 in water. Both cases have been implemented and simulated in FEM tool COMSOL Multiphysics®. From the comparison of resulting SO_2 concentrations at the inlet to the dryer and the final concentrations at the outlet from the dryer it follows that the SO_2 loses can be significant for the measurements using P-AMSs. However, more detailed numerical analysis and comparison with experimental findings should be done for validation of this conclusion.

Acknowledgement

The author acknowledges the support received from the European Metrology Programme for Innovation and Research (EMPIR) through the Joint Research Project "Metrology for Sampling and Conditioning SO2 Emissions from Stacks". The EMPIR is jointly funded by the European Commission and participating countries within Euramet and the European Union.

References

[1] F. Derriennic, S. Richardson, A. Mollie a J. Lellouch, „Short-term effect of sulphur dioxide pollution on mortality in two French cities," *International Journal of Epidemiology*, pp. 186-197, March 1989.

[2] [Online].Available: http://www.learsiegler.com.au/suppliers/mc/PSS.html. [16/5/2019].

[3] W. C. Hinds, Aerosol Technology, New York: John Wiley & Sons, Inc., 1999.

[4] A. Faghri a Y. Zhang, Transport Phenomena in Multiphase Systems, London: Academic Press, Elsevier Inc., 2006.

[5] A. Faghri, „Turbulent Film Condensation in a Tube with Concurrent and Countercurrent Vapor Flow," v *AIAA/ASME 4th Joint Thermophysics and Heat Transfer Conference*, Boston, 1986.

[6] S. Thumm, C. Philipp a U. Gross, „Film condensation of water in a vertical tube with countercurrent vapour flow," *International Journal of Heat and Mass Transfer 44*, pp. 4245-4256, 2001.

[7] R. A. Seban a J. A. Hodgson, „Laminar film condensation in a tube with upward vapor flow," *International Journal of Heat and Mass Transfer, Vol. 25, No. 9*, pp. 1291-1300, 1982.

[8] N. Samkhaniani a M. R. Ansari, „The evaluation of the diffuse interface method for phase change simulations using OpenFOAM," *Heat transfer - Asian Res*, pp. 1-31, 2017.

[9] M. K. Groff, S. J. Ormiston a H. M. Soliman, „Numerical solution of film condensation from turbulent flow of vapor-gas mixtures in vertical tubes," *International Journal of Heat and Mass Transfer, 50*, pp. 3899-3912, 2007.

[10] M. Nitche a R. O. Gbadamosi, Heat exchanger design guide. A practical Guide for planning, Selecting and Design of Shell and Tube Exchangers, London: Butterworth Heinnemann, Elsevier, 2016.

[11] N. Zhang, J. Zhang, Y. Zhang, J. Bai a X. Wei, „Solubility and Henry's law constant of sulfur dioxide in aqueous polyethylene glycol 300 solution at different temperatures ans pressures," *Fluid Phase Equilibria, 348*, pp. 9-16, 2013.

[12] R. Sander, „Compilation of Henry's law constants (version 4.0) for water as solvent," *Atmospheric Chemistry and Physics, 15*, pp. 4399-4981, 2015.

[13] J. L. Ponche, C. George a P. Mirabel, „Mass Transfer at the Air/Water Interfrace: Mass Accommodation Coefficients of SO2, HNO3, NO2 and NH3," *Journal of Atmospheric Chemistry, 16*, pp. 1-21, 1993.

[14] J. A. Gardner, L. R. Watson, Y. G. Adewuyi, P. Davidovits, M. S. Zahniser, D. R. Worsnop a C. E. Kolb, „Measurement of the Mass Accommodation Coefficient of SO2 (g) on Water Droplets," *Journal of Geophysical Research, vol. 92, No. D9*, pp. 10887-10895, 20 September 1987.

[15] T. Elperin, A. Fominykh a B. Krasovitov, „Scavenging of soluble gases by evaporating and growing cloud droplets in the presence of aqueous-phase dissociation reaction," *Atmospheric Environment, 42*, pp. 3076-3086, 2008.

[16] M. K. Mondal, „Experimental determination of dissociation constant, Henry's constant, heat of reactions, SO2 absorbed and gas bubble-liquid interfacial area for dilute sulphur dioxide absorption into water," *Fluid Phase Equilibria, 253*, pp. 98-107, 2007.

[17] A. Koliadima, J. Kapalos a L. Farmakis, „Diffusion Coefficients of SO2 in Water and Partition Coeffiecient of SO2 in Water-Air Interface at Different Temperature and pH Values," *Instrumentation Science & Technology, 37:3*, pp. 274-283, 21 April 2009.

[18] J. Crank, The Mathematics of Diffussion, Oxford: Clarendon Press, 1975.

[19] T. Huthwelker a T. Peter, „Analytical description of gas transport across an interface with coupled diffusion in two phases," *J. Chem. Phys, 105, (4)*, pp. 1661-1667, 22 July 1996.

[20] J. O. Hirschfelder, C. F. Curtiss a R. B. Bird, Molecular Theory of Gases and Liquids, New York: Wiley, 1954.

[21] T. Elperin, A. Fominykh a B. Krasovitov, „Evaporation and Condensation of Large Droplets in the Presence of Inert Admixtures Containing Soluble Gas," *Journal of the Atmospheric Sciences*, pp. 983-995, March 2007.

[22] M. P. Perujo, „Condensation of Water Vapor and Acid Mixtures from Exhaust Gases, PhD Thesis," Technische Universität Berlin, Berlin, 2004.

[23] E. Serris, M. Cournil a J. Peultier, „Modeling and simulation of acid gas condensation in an industrial chimney," *International Journal of Chemical Reactor Engineering, De Gruyter*, p. pp.A39, 2009.

[24] H. G. Maahs, „Sulfur-dioxide/water equilibria between 0° and 50°C. An examination of data at low concentrations," v *Heterogeneous Atmospheric Chemistry, Geophysical Monograph, 26*, S. D. R., Editor, Washington, D.C., Am. Geophys. Union, 1982, pp. 187-195.